

Bromide complexes of bismuth with 4-bromobenzyl-substituted cations of pyridinium family



Igor D. Gorokh ^{a, b}, Sergey A. Adonin ^{a, c, d, *}, Andrey N. Usoltsev ^a, Alexander S. Novikov ^e, Denis G. Samsonenko ^{a, f}, Sergey V. Zakharov ^g, Maxim N. Sokolov ^{a, f, h}, Vladimir P. Fedin ^{a, f}

^a Nikolaev Institute of Inorganic Chemistry SB RAS, 630090, 3 Lavrentiev Av., Novosibirsk, Russia

^b Skolkovo Institute of Science and Technology, Center for Electrochemical Energy Storage, 143026, Nobel St. 3, Moscow, Russia

^c Tobolsk Industrial Institute (Branch of Tyumen Industrial University), 626158, Zona Vuzov 5, Tobolsk, Russia

^d South Ural State University, Chelyabinsk, 454080, Russia

^e Saint Petersburg State University, Institute of Chemistry, 199034, Universitetskaya Nab. 7-9, Saint Petersburg, Russia

^f Novosibirsk State University, 630090, Pirogova St. 2, Novosibirsk, Russia

^g Irkutsk National Research Technical University, 664074, Lermontov St. 83, Irkutsk, Russia

^h Kazan Federal University, Alexander Butlerov Institute of Chemistry, Lobachevskogo St. 1/29, 420008, Kazan, Russia

ARTICLE INFO

Article history:

Received 9 April 2019

Received in revised form

19 August 2019

Accepted 19 August 2019

Available online 20 August 2019

Keywords:

Halide complexes

Hirshfeld surface analysis

Bismuth

Supramolecular contacts

ABSTRACT

Two bromobismuthate (III) complexes containing 4-bromobenzyl-substituted pyridinium cations – $(1-(4-\text{BrBz})\text{Py})_3[\text{Bi}_2\text{Br}_9]$ (**1**) and $(1-(4-\text{BrBz})-2-\text{MePy})_3[\text{BiBr}_6]$ (**2**) – were prepared by reactions of Bi_2O_3 and corresponding pyridinium bromides in HBr. In the structure of **1** there are weak contacts between the Br atoms of $1-(4-\text{BrBz})\text{Py}^+$ and bromide ligands of $[\text{Bi}_2\text{Br}_9]^{3-}$, while in the case of **2** such interactions are absent. The contributions of halogen and hydrogen bonding were estimated by Hirshfeld surface analysis (HSA); additionally, energies of $\text{Br}\cdots\text{Br}$ type I halogen-halogen contacts were calculated.

© 2019 Elsevier B.V. All rights reserved.

1. Introduction

Anionic halide complexes of p-block elements have moved close to the center stage of current coordination chemistry. The activity in this field is stimulated by peculiar physical properties of the compounds in this class, such as photocatalytic activity (especially for Cu and Ag complexes) [1–3], unusual solvent-induced color changes [4], luminescence [5–7], ferroelectric behaviour [8–14] etc. One of the most prominent topics is the use of halide (first of all, iodide) complexes as light absorbers in solar cells [15–20]. For this area, there are several crucial parameters which must be achieved; those are: 1) thermal and photostability, 2) lower optical band gap and 3) preferably structure of higher dimensionality in order to achieve isotropy. Since controllable preparation of halometalates

with certain molecular structure remains a challenging task (and it is unclear whether such synthetic approaches can be found), screening remains the key method for the search of compounds with desired properties. Recently we reported [21] that halobismuthate (III) complexes with halogen-substituted cations of pyridinium family can demonstrate unusual optical behaviour due to formation of halogen-halogen short contacts in solid state. In order to check whether such effects are expandable on the complexes with other aromatic cations able to form halogen-halogen short contacts in solid state, we used 4-bromobenzyl-substituted Py derivatives. We consider both type I interactions which assumed to appear due to crystal packing effects and type II interactions (“classic” halogen bonding (XB)). In this work we report two new bromobismuthates (III) – $(1-(4-\text{BrBz})\text{Py})_3[\text{Bi}_2\text{Br}_9]$ (**1**) and $(1-(4-\text{BrBz})-2-\text{MePy})_3[\text{BiBr}_6]$ (**2**) and discuss the features of supramolecular contacts in their structures.

* Corresponding author. Nikolaev Institute of Inorganic Chemistry SB RAS, 630090, 3 Lavrentiev av., Novosibirsk, Russia.

E-mail address: adonin@niic.nsc.ru (S.A. Adonin).

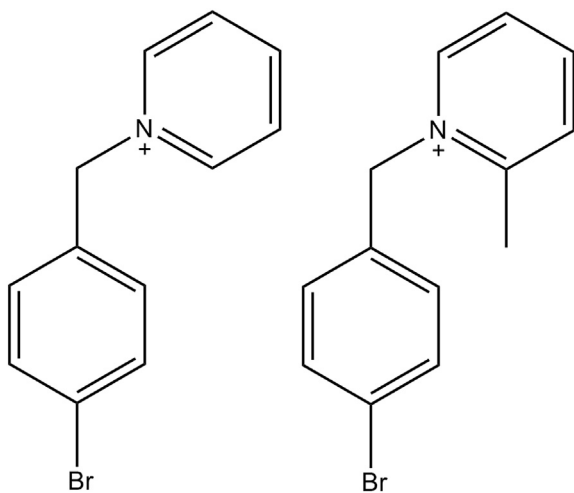


Fig. 1. Structures of $1\text{-}(4\text{-BrBz})\text{Py}^+$ (left) and $1\text{-}(4\text{-BrBz})\text{-2-MePy}^+$ (right) cations.

2. Experimental part

All experiments were carried out in air. $1\text{-}(4\text{-bromobenzyl})\text{pyridinium}$ and $1\text{-}(4\text{-bromobenzyl})\text{-2-methylpyridinium}$ (Fig. 1) bromides were prepared by reactions of pyridine or 2-picoline with 4-bromobenzyl bromide (1:1.1) in acetonitrile (24 h, r.t., yields are close to quantitative). Elemental analysis was performed on a Euro NA 3000 Elemental Analyzer (EuroVector).

Synthesis of $(1\text{-}(4\text{-BrBz})\text{Py})_3[\text{Bi}_2\text{Br}_9]$ (1). 43 mg (0.099 mmol) of Bi_2O_3 were dissolved in 15 ml 2 M HBr; then solution of $1\text{-}(4\text{-BrBz})\text{PyBr}$ (90 mg, 0.276 mmol) in 15 ml of 2 M HBr was added. Within 1 day, there form pale yellow crystals of 1. Yield 79%. For $\text{C}_{36}\text{H}_{33}\text{N}_3\text{Bi}_2\text{Br}_{12}$ calcd, %: C, 23.1; H, 1.8; N, 2.2; found, %: C, 23.0; H, 1.8; N, 2.2.

Synthesis of $(1\text{-}(4\text{-BrBz})\text{-2-MePy})_3[\text{Bi}_2\text{Br}_9]$ (2). 15 mg (0.032 mmol) of Bi_2O_3 were dissolved in 10 ml of 2 M HBr; then solution of $1\text{-}(4\text{-BrBz})\text{-2-MePyBr}$ (16 mg, 0.048 mmol) in 8 ml of

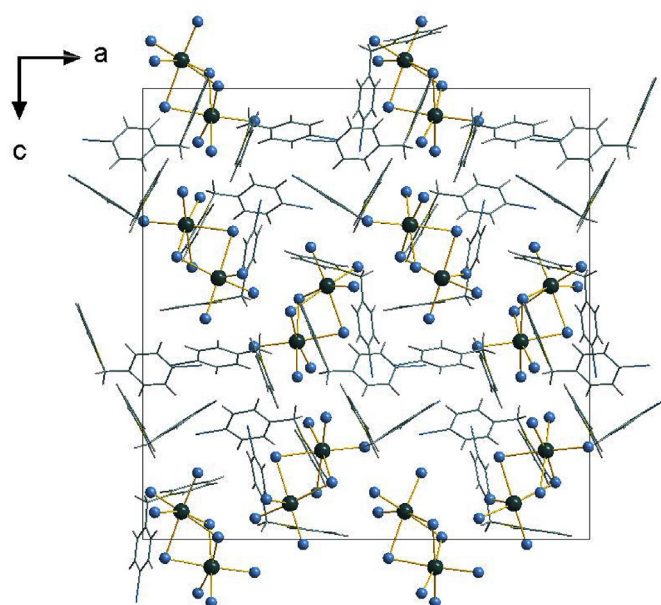


Fig. 2. Crystal packing in the structure of 1.

HBr was added. Within 1 day, there form pale yellow crystals of 2. Yield 81%. For $\text{C}_{39}\text{H}_{39}\text{N}_3\text{BiBr}_9$ calcd, %: C, 31.9; H, 2.7; N, 2.9; found, %: C, 31.8; H, 2.7; N, 2.8.

X-ray Diffractometry. Diffraction data for single crystals 1 and 2 were obtained at 130 K on an automated Agilent Xcalibur diffractometer equipped with an area AtlasS2 detector (graphite monochromator, $\lambda(\text{MoK}\alpha) = 0.71073 \text{ \AA}$, ω -scans). Integration, absorption correction, and determination of unit cell parameters were performed using the CrysAlisPro program package (CrysAlisPro 1.171.38.41. Rigaku Oxford Diffraction: The Woodlands, TX, USA, 2015). The structures were solved by dual space algorithm (SHELXT) [22] and refined by the full-matrix least squares technique (SHELXL) [23] in the anisotropic approximation (except

Table 1
Crystal data and structure refinement for 1 and 2.

Compound	1	2
Empirical formula	$\text{C}_{36}\text{H}_{33}\text{Bi}_2\text{Br}_{12}\text{N}_3$	$\text{C}_{39}\text{H}_{39}\text{BiBr}_9\text{N}_3$
M, g/mol	1884.53	1477.90
Crystal system	<i>Orthorhombic</i>	<i>Monoclinic</i>
Space group	Pca_2_1	$P2_1/n$
a, Å	27.3642(13)	15.4597(5)
b, Å	12.6778(5)	17.1922(4)
c, Å	27.5745(13)	18.5102(6)
α , deg.	90	90
β , deg.	90	113.447(4)
γ , deg.	90	90
V, \AA^3	9566.1(7)	4513.5(3)
Z	8	4
D(calcd), g/cm ³	2.617	2.175
μ , mm ⁻¹	17.403	11.905
F(000)	6848	2768
Crystal size, mm	$0.24 \times 0.17 \times 0.05$	$0.39 \times 0.33 \times 0.28$
θ range for data collection, deg.	3.36–25.35	3.30–28.97
Index ranges	$-20 \leq h \leq 32, -15 \leq k \leq 10, -33 \leq l \leq 25$	$-15 \leq h \leq 21, -22 \leq k \leq 23, -23 \leq l \leq 19$
Reflections collected/independent	24993/13443	37580/10442
R_{int}	0.0449	0.0286
Reflections with $I > 2\sigma(I)$	12243	8877
Goodness-of-fit on F^2 [2]	1.031	1.036
Final R indices [$I > 2\sigma(I)$]	$R_1 = 0.0415, wR_2 = 0.0930$	$R_1 = 0.0247, wR_2 = 0.0460$
R indices (all data)	$R_1 = 0.0486, wR_2 = 0.0963$	$R_1 = 0.0351, wR_2 = 0.0480$
Largest diff. peak/hole, e/Å ³	1.398/−1.138	1.249/−1.131

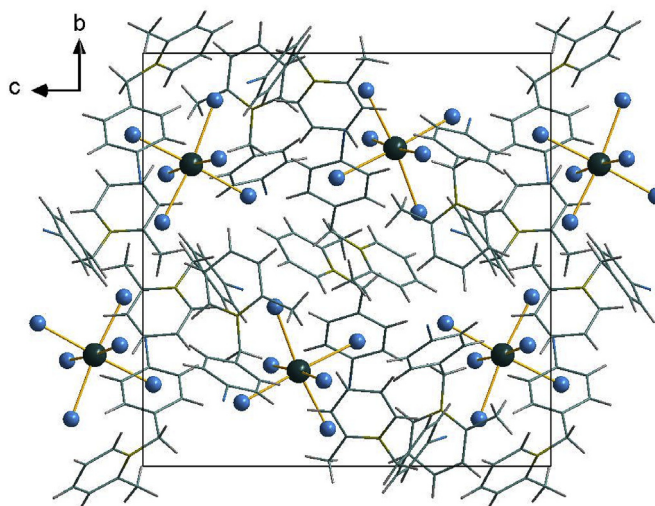


Fig. 3. Crystal packing in the structure of **2**.

hydrogen atoms). Positions of hydrogen atoms of organic ligands were calculated geometrically and refined in the riding model. Residual density on Bi and Br does not exceed the limits common for heavier atoms. The crystallographic data and details of the structure refinements are summarized in **Table 1**. CCDC 1908927–1908928 contain the supplementary crystallographic data for this paper. These data can be obtained free of charge from

The Cambridge Crystallographic Data Center at http://www.ccdc.cam.ac.uk/data_request/cif.

3. Results and discussion

According to the Cambridge Structural Database (CSD), there are over ten crystal structures containing 1-(4-bromobenzyl)pyridinium cation [24–27]. One of those (CCDC 811817) contains $[\text{CuBr}_4]^{2-}$ as a counter anion. Our scrutiny did not detect $\text{Br}\cdots\text{Br}$ interactions classifiable as halogen-halogen short contacts. In all cases these distances exceed 3.66 Å, which is the sum of Bondi's van der Waals radii for two Br atoms [28,29]. Structures with 1-(4-bromobenzyl)-2-methylpyridinium have not been reported.

In the structure of **1**, the anionic part consists of well-known [11,12,30–37] binuclear $[\text{Bi}_2\text{Br}_9]^{3-}$ units. The Bi–Br bond lengths are within the usual range ($\text{Bi} - \text{Br}_{\text{term}} = 2.675\text{--}2.803$ Å; $\text{Bi} - \mu_2\text{-Br} = 2.947\text{--}3.162$ Å, respectively). The search for possible $\text{Br}\cdots\text{Br}$ contacts revealed that relevant distances are only slightly under the sum of van der Waals radii (3.648 Å in **1** vs 3.66 Å for two Br van der Waals radii), indicating weak interactions between the Br atoms of 4-bromobenzyl units and terminal Br ligands. The shortest H···Br contacts in **1** are 2.765 Å, and these involve $\mu_2\text{-Br}$ and CH_2 fragment of cation, while the contacts with Br_{term} are longer; similar effects were found in other structures of $[\text{Bi}_2\text{Br}_9]^{3-}$ salts [38]. The crystal packing in **1** is shown in **Fig. 2** (additional figures illustrating H···Br and Br···Br contacts are given in SI). The bromobismuthate units in **2** are mononuclear $[\text{BiBr}_6]^{3-}$ (**Fig. 3**) with slightly distorted octahedral geometry at Bi ($\text{Bi}-\text{Br} = 2.786\text{--}2.923$ Å). The shortest H···Br

Table 2
Results of the HSA for the X-ray structures of **1** and **2**.

X-ray structure	Contributions of different intermolecular contacts to the molecular Hirshfeld surface ^a
1	Anionic part: Br–H 90.5%, Br–C 5.0%, Br–Br 4.1% Cationic part: Br–H 44.9%, H–H 18.3%, C–H 16.9%, Br–C 12.9%, C–C 3.8%, Br–Br 1.4%, N–C 1.3%
2	Anionic part: Br–H 91.7%, Br–C 6.0%, Br–N 1.6% Cationic part: H–H 38.5%, Br–H 31.9%, C–H 17.0%, Br–C 6.0%, C–C 4.8%, N–H 1.2%

^a The contributions of all other intermolecular contacts do not exceed 1%.

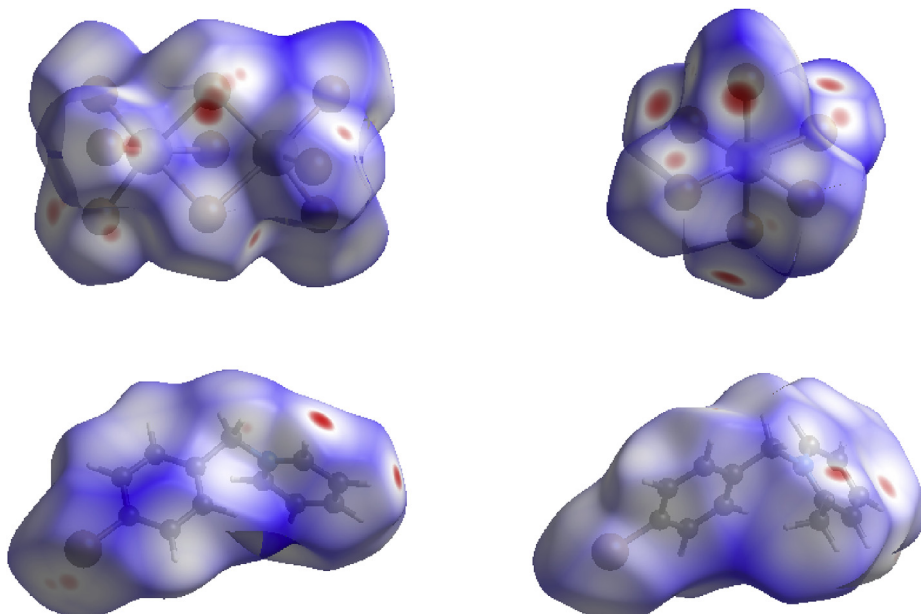


Fig. 4. Hirshfeld surfaces for **1** (left) and **2** (right) (anionic and cationic parts).

Table 3

Values of the density of all electrons ($\rho(\mathbf{r})$), Laplacian of electron density ($\nabla [2]\rho(\mathbf{r})$) and appropriate λ_2 eigenvalue, energy density (H_b), potential energy density ($V(\mathbf{r})$), and Lagrangian kinetic energy ($G(\mathbf{r})$) (a.u.) at the bond critical point (3, -1), corresponding to non-covalent interactions Br···Br (type I halogen-halogen short contacts) in supramolecular structure of **1**, bond length (l) (Å), Wiberg bond index (WI), as well as energy for this contact E_{int} (kcal/mol), defined by different approaches.

$\rho(\mathbf{r})$	$\nabla [2]\rho(\mathbf{r})$	λ_2	H_b	$V(\mathbf{r})$	$G(\mathbf{r})$	E_{int}^a	E_{int}^b	E_{int}^c	E_{int}^d	l^e	WI
0.007	0.018	-0.008	0.000	-0.004	0.004	1.3	1.1	1.5	1.4	3.647	0.01

^a $E_{int} = -V(\mathbf{r})/2^{53}$.

^b $E_{int} = 0.429G(\mathbf{r})$ [54].

^c $E_{int} = 0.58(-V(\mathbf{r}))$ (correlation developed exclusively for non-covalent interactions involving bromine atoms) [55].

^d $E_{int} = 0.57G(\mathbf{r})$ (correlation developed exclusively for non-covalent interactions involving bromine atoms) [54].

^e The shortest van der Waals radius for Br atom is 1.83 Å²⁹.

contacts are 2.710 Å (with H atoms of phenyl rings), and the Br···Br distances exceed the sum of corresponding van der Waals radii, indicating lack of such interactions. Both complexes were isolated as pure phases, according to the PXRD data (see SI).

For estimation of relative contributions of different contacts to the crystal packing, we performed Hirshfeld surface analysis (HSA) for **1** and **2**, see Table 2 and SI for details. For the visualization, we have used a mapping of the normalized contact distance (d_{norm}); its negative value enables identification of molecular regions of substantial importance for detection of short contacts. Fig. 4 depicts the Hirshfeld surfaces for **1** and **2** (anionic and cationic parts). In these Hirshfeld surfaces, the regions of shortest intermolecular contacts visualized by red circle areas. In both cases, the dominating contacts are Br···H and/or H···H (this situation is common for halometalates [39,40]); however, in the case of **1**, contribution of abovementioned Br···Br interactions (type I halogen-halogen short

contacts [41,42]) takes place as well.

For estimation of the energies of these type I halogen-halogen short contacts which, in our opinion, are related to the phenomenon of halogen bonding [41,42], we performed DFT calculations and topological analysis of the electron density distribution (QTAIM theory) [43] for **1**. Previously, this approach was successfully utilized for the studies of various non-covalent interactions in coordination compounds [44–51]. Results are summarized in Table 3, the contour line diagram of the Laplacian distribution $\nabla [2]\rho(\mathbf{r})$, bond paths, and selected zero-flux surfaces as well as reduced density gradient (RDG) isosurface [52] for non-covalent interactions Br···Br in supramolecular structure of **1** are shown in Fig. 5.

The Laplacian of electron density is typically decomposed into the sum of contributions along the three principal axes of maximal variation, giving the three eigen values (λ_1, λ_2 and λ_3) of the Hessian matrix. In line with common practice, the sign of λ_2 can be utilized to distinguish bonding (attractive, $\lambda_2 < 0$) weak interactions from non-bonding ones (repulsive, $\lambda_2 > 0$). Thus, the discussed above non-covalent interactions Br···Br (type I halogen-halogen short contacts) in supramolecular structure of **1** are attractive (Table 3).

The QTAIM analysis demonstrates the presence of appropriate bond critical point (3, -1) (BCP) for non-covalent interactions Br···Br in supramolecular structure of **1** (Table 3). The low magnitude of the electron density, positive value of the Laplacian, and very low energy density in this BCP are typical for non-covalent interactions involving halogen atoms [56,57]. We have defined energy for this weak contact Br···Br according to several procedures [53–55]; depending on the approach used, the strength of this contact vary in the ranges 1.1–1.5 kcal/mol. The balance between the Lagrangian kinetic energy $G(\mathbf{r})$ and potential energy density $V(\mathbf{r})$ at the BCP reveals that a covalent contribution is absent in Br···Br supramolecular contacts in **1** [58], which correlates well with negligible Wiberg bond indices for these interactions. The NBO charges on the bromine atoms involving in non-covalent interactions Br···Br in supramolecular structure of **1** are -0.44 (anionic part) and 0.12 (cationic part).

Overall, analysis of both geometries and energies of Br···Br interactions reveals that those should be rather classified as Type I halogen···halogen short contacts according to the classification by Metrangolo et al.

According to the TGA data (see SI), both **1** and **2** reveal high thermal stability (decomposition begins at ≈ 200 °C for **1** and ≈ 220 °C for **2**). These observations agree well with the investigations of thermal stability of bromobismuthates(III) made by us earlier [59].

4. Conclusions

With 4-bromobenzyl-substituted pyridinium salts as precursors, we prepared two new bromobismuthate complexes. Combination of Hirshfeld Surface Analysis (HSA) and DFT show that

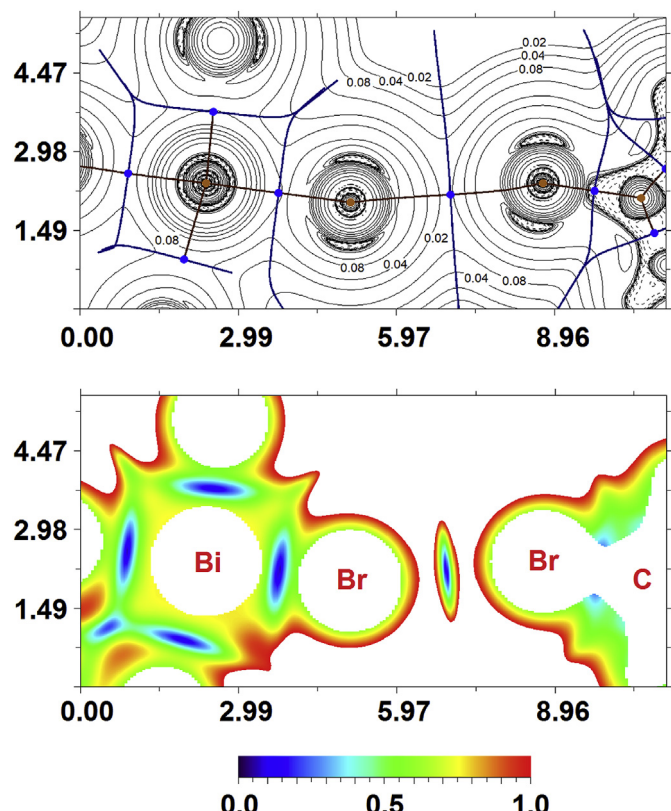


Fig. 5. Contour line diagram of the Laplacian distribution $\nabla [2]\rho(\mathbf{r})$, bond paths and selected zero-flux surfaces (top) and RDG isosurface (bottom) referring to non-covalent interactions Br···Br in **1** (packing induced contact aka type I halogen-halogen short contact). Bond critical points (3, -1) are shown in blue, nuclear critical points (3, -3) – in pale brown, length units – Å, isovalues on contour lines and RDG isosurface values on the color scheme are given in a.u.

the desired Br···Br contacts indeed appear in the solid state, but their role in crystal packing is minor and their energies are low. From the point of view of halometalate crystal engineering, halogen-substituted pyridiniums [21,60] still remain better candidate for XB formation because of higher charge anisotropy of bromide atom bounded to electron deficientpyridinium moiety.

Acknowledgements

This work was supported by Russian Science Foundation (Grant No. 18-73-10040).

Appendix A. Supplementary data

Supplementary data to this article can be found online at <https://doi.org/10.1016/j.molstruc.2019.126955>.

References

- [1] X.-W. Lei, C.-Y. Yue, F. Wu, X.-Y. Jiang, L.-N. Chen, Inorg. Chem. Commun. 77 (2017) 64–67.
- [2] X.-W. Lei, C.-Y. Yue, J.-C. Wei, R.-Q. Li, F.-Q. Mi, Y. Li, L. Gao, Q.-X. Liu, Chem. Eur. J. 23 (2017) 14547–14553.
- [3] K.-B. Chu, J.-L. Xie, W.-J. Chen, W.-X. Lu, J.-L. Song, C. Zhang, Polyhedron 151 (2018) 146–151.
- [4] B. Wagner, N. Dehnhardt, M. Schmid, B.P. Klein, L. Ruppenthal, P. Müller, M. Zugermeier, J.M. Gottfried, S. Lippert, M.-U. Halbich, A. Rahimi-Iman, J. Heine, J. Phys. Chem. C 120 (2016) 28363–28373.
- [5] J.C. Ahern, A.D. Nicholas, A.W. Kelly, B. Chan, R.D. Pike, H.H. Patterson, Inorg. Chim. Acta 478 (2018) 71–76.
- [6] A.W. Kelly, A. Nicholas, J.C. Ahern, B. Chan, H.H. Patterson, R.D. Pike, J. Alloy. Comp. 670 (2016) 337–345.
- [7] J.R. Sorg, T. Wehner, P.R. Matthes, R. Sure, S. Grimme, J. Heine, K. Müller-Buschbaum, Dalton Trans. 47 (2018) 7669–7681.
- [8] M. Węcławik, A. Gągor, R. Jakubas, A. Piecha-Bisiorek, W. Medycki, J. Baran, P. Zieliński, M. Gałażka, Inorg. Chem. Front. 3 (2016) 1306–1316.
- [9] A. Piecha-Bisiorek, R. Jakubas, W. Medycki, M. Florek-Wojciechowska, M. Wojciechowski, D. Kruk, J. Phys. Chem. A 118 (2014) 3564–3571.
- [10] M. Chański, A. Bialońska, R. Jakubas, A. Piecha-Bisiorek, Polyhedron 71 (2014) 69–74.
- [11] P. Szklarz, R. Jakubas, A. Piecha-Bisiorek, G. Bator, M. Chański, W. Medycki, J. Wuttke, Polyhedron 139 (2018) 249–256.
- [12] M. Wojtaś, R. Jakubas, J. Baran, Vib. Spectrosc. 39 (2005) 23–30.
- [13] B. Kulicka, R. Jakubas, A. Pietraszko, G. Bator, J. Baran, Solid State Sci. 6 (2004) 1273–1286.
- [14] A. Piecha, R. Jakubas, V. Kinzhbalo, T. Lis, J. Mol. Struct. 887 (2008) 194–200.
- [15] L.A. Frolova, D.V. Anokhin, A.A. Piryazev, S.Y. Luchkin, N.N. Dremova, P.A. Troshin, J. Phys. Chem. Lett. 8 (2017) 1651–1656.
- [16] L.A. Frolova, D.V. Anokhin, A.A. Piryazev, S.Y. Luchkin, N.N. Dremova, K.J. Stevenson, P.A. Troshin, J. Phys. Chem. Lett. 8 (2017) 67–72.
- [17] L.A. Frolova, N.N. Dremova, P.A. Troshin, Chem. Commun. 51 (2015) 14917–14920.
- [18] A.M. Ganose, C.N. Savory, D.O. Scanlon, Chem. Commun. 53 (2017) 20–44.
- [19] T.A. Shestimerova, N.A. Yelavik, A.V. Mironov, A.N. Kuznetsov, M.A. Bykov, A.V. Grigorieva, V.V. Utocnikova, L.S. Lepnev, A.V. Shevelkov, Inorg. Chem. 57 (2018) 4077–4087.
- [20] T.A. Shestimerova, N.A. Golubev, N.A. Yelavik, M.A. Bykov, A.V. Grigorieva, Z. Wei, E.V. Dikarev, A.V. Shevelkov, Cryst. Growth Des. 18 (2018) 2572–2578.
- [21] S.A. Adonin, I.D. Gorokh, A.S. Novikov, D.G. Samsonenko, I.V. Yushina, M.N. Sokolov, V.P. Fedin, CrystEngComm 20 (2018) 7766–7772.
- [22] G.M. Sheldrick, Acta Crystallogr. Sect. C Struct. Chem. 71 (2015) 3–8.
- [23] C.B. Hübschle, G.M. Sheldrick, B. Dittrich, J. Appl. Crystallogr. 44 (2011) 1281–1284.
- [24] X.M. Ren, H. Okudera, R.K. Kremer, Y. Song, C. He, Q.J. Meng, P.H. Wu, Inorg. Chem. 43 (2004) 2569–2576.
- [25] X. Ren, Q. Meng, Y. Song, C. Lu, C. Hu, X. Chen, Inorg. Chem. 41 (2002) 5686–5692.
- [26] X. Ren, J. Ma, C. Lu, S. Yang, Q. Meng, P. Wu, Dalton Trans. (2003) 1345–1351.
- [27] C. Ni, D. Dang, Z. Ni, Y. Li, J. Xie, Q. Meng, Y. Yao, J. Coord. Chem. 57 (2004) 1529–1536.
- [28] M. Mantina, A.C. Chamberlin, R. Valero, C.J. Cramer, D.G. Truhlar, J. Phys. Chem. A 113 (2009) 5806–5812.
- [29] A. Bondi, J. Phys. Chem. 70 (1966) 3006–3007.
- [30] M. Wojtaś, R. Jakubas, Z. Ciunik, W. Medycki, J. Solid State Chem. 177 (2004) 1575–1584.
- [31] I.A. Ahmed, R. Blachnik, G. Kastner, W. Brockner, Z. Anorg. Allg. Chem. 627 (2001) 2261.
- [32] B. Ptaszyński, Thermochim. Acta 197 (1992) 479–490.
- [33] G.A. Bowmaker, P.C. Junk, A.M. Lee, B.W. Skelton, A.H. White, Aust. J. Chem. 51 (1998) 293.
- [34] Y.-H. Peng, S.-F. Sun, X.-H. Yang, T. Gao, Y. Li, J. Wang, J. Mol. Struct. 1056–1057 (2014) 202–208.
- [35] V.V. Sharutin, I.V. Yegorova, N.N. Klepikov, E.A. Boyarkina, O.K. Sharutina, Russ. J. Inorg. Chem. 54 (2009) 52–68.
- [36] W.-X. Chai, J. Lin, L. Song, L.-S. Qin, H.-S. Shi, J.-Y. Guo, K.-Y. Shu, Solid State Sci. 14 (2012) 1226–1232.
- [37] G.A. Bowmaker, J.M. Harrowfield, P.C. Junk, B.W. Skelton, A.H. White, Aust. J. Chem. 51 (1998) 285.
- [38] S.A. Adonin, I.D. Gorokh, D.G. Samsonenko, O.V. Antonova, I.V. Korolkov, M.N. Sokolov, V.P. Fedin, Inorg. Chim. Acta 469 (2018), 32–27.
- [39] O. Ben Moussa, H. Chebbi, M.F. Zid, J. Mol. Struct. 1180 (2019) 72–80.
- [40] Z. Ouerghi, T. Roisnel, R. Fezai, R. Kefi, J. Mol. Struct. 1173 (2018) 439–447.
- [41] G. Cavallo, P. Metrangolo, T. Pilati, G. Resnati, M. Sansotera, G. Terraneo, Chem. Soc. Rev. 39 (2010) 3772.
- [42] G. Cavallo, P. Metrangolo, R. Milani, T. Pilati, A. Priimagi, G. Resnati, G. Terraneo, Chem. Rev. 116 (2016) 2478–2601.
- [43] R.F.W. Bader, Chem. Rev. 91 (1991) 893–928.
- [44] X. Ding, M.J. Tuikkä, P. Hirva, V.Y. Kukushkin, A.S. Novikov, M. Haukka, CrystEngComm 18 (2016) 1987–1995.
- [45] A.S. Novikov, Inorg. Chim. Acta 471 (2018) 126–129.
- [46] D.M. Ivanov, A.S. Novikov, I.V. Ananyev, V.Y. Kirina, V.Y. Kukushkin, Chem. Commun. 52 (2016) 5565–5568.
- [47] D.M. Ivanov, M.A. Kinzhalov, A.S. Novikov, I.V. Ananyev, A.A. Romanova, V.P. Boyarskiy, M. Haukka, V.Y. Kukushkin, Cryst. Growth Des. 17 (2017) 1353–1362.
- [48] L.E. Zelenkov, D.M. Ivanov, M.S. Avdonteveva, A.S. Novikov, N.A. Bokach, Z. Krist. - Cryst. Mater. 234 (2019) 9–17.
- [49] E.V. Andrusenko, A.S. Novikov, G.L. Starova, N.A. Bokach, Inorg. Chim. Acta 447 (2016) 142–149.
- [50] M. Bulatova, A.A. Melekhova, A.S. Novikov, D.M. Ivanov, N.A. Bokach, Z. Krist. - Cryst. Mater. 233 (2018) 371–377.
- [51] Z.M. Bikbaeva, D.M. Ivanov, A.S. Novikov, I.V. Ananyev, N.A. Bokach, V.Y. Kukushkin, Inorg. Chem. 56 (2017) 13562–13578.
- [52] E.R. Johnson, S. Keinan, P. Mori-Sánchez, J. Contreras-García, A.J. Cohen, W. Yang, J. Am. Chem. Soc. 132 (2010) 6498–6506.
- [53] E. Espinosa, E. Molins, C. Lecomte, Chem. Phys. Lett. 285 (1998) 170–173.
- [54] M.V. Vener, A.N. Egorova, A.V. Churakov, V.G. Tsirelson, J. Comput. Chem. 33 (2012) 2303–2309.
- [55] E. V. Bartashevich, V.G. Tsirelson, Russ. Chem. Rev. 83 (2014) 1181–1203.
- [56] A.S. Novikov, D.M. Ivanov, Z.M. Bikbaeva, N.A. Bokach, V.Y. Kukushkin, Cryst. Growth Des. 18 (2018) 7641–7654.
- [57] S.V. Baykov, U. Dabrowskaya, D.M. Ivanov, A.S. Novikov, V.P. Boyarskiy, Cryst. Growth Des. 18 (2018) 5973–5980.
- [58] E. Espinosa, I. Alkorta, J. Elguero, E. Molins, J. Chem. Phys. 117 (2002) 5529–5542.
- [59] S.A. Adonin, I.D. Gorokh, D.G. Samsonenko, A.S. Novikov, I.V. Korolkov, P.E. Plyusnin, M.N. Sokolov, V.P. Fedin, Polyhedron 159 (2019) 318–322.
- [60] V. Gómez, O. Fuhr, M. Ruben, CrystEngComm 18 (2016) 8207–8219.